Supporting Information

Nitrogen-doped $NiCo_2O_4$ Microsphere as an Efficient Catalyst for Flexible Rechargeable Zinc-Air Batteries and Self-charging Power System

Juanjuan Bian,[1,2‡] Xiaopeng Cheng,[3‡] Xiaoyi Meng,[1,2] Jian Wang,[4] Jigang Zhou,[4] Shaoqing Li,[1,2] Yuefei Zhang,[3*] and Chunwen Sun[1,2,5*]

[1]CAS Center for Excellence in Nanoscience, Beijing Institute of Nanoenergy and Nanosystems, Chinese Academy of Sciences, Beijing 100083, P. R. China

[2]School of Nanoscience and Technology, University of Chinese Academy of Sciences, Beijing 100049, P. R. China

[3]Institute of Microstructure and Property of Advanced Materials, Beijing University of Technology, Beijing 100124, P.R. China

[4]Canadian Light Source Inc., University of Saskatchewan, Saskatoon, SK S7N 2V3, Canada

[5]Center on Nanoenergy Research, School of Physical Science and Technology, Guangxi University, Nanning 530004, P.R. China

[*] Corresponding authors.

Tel.: +86-10-82854648, fax: +86-10-82854648. Email: yfzhang@bjut.edu.cn (Y.F. Zhang), sunchunwen@binn.cas.cn (C. Sun)

‡ These authors contributed equally to this work.

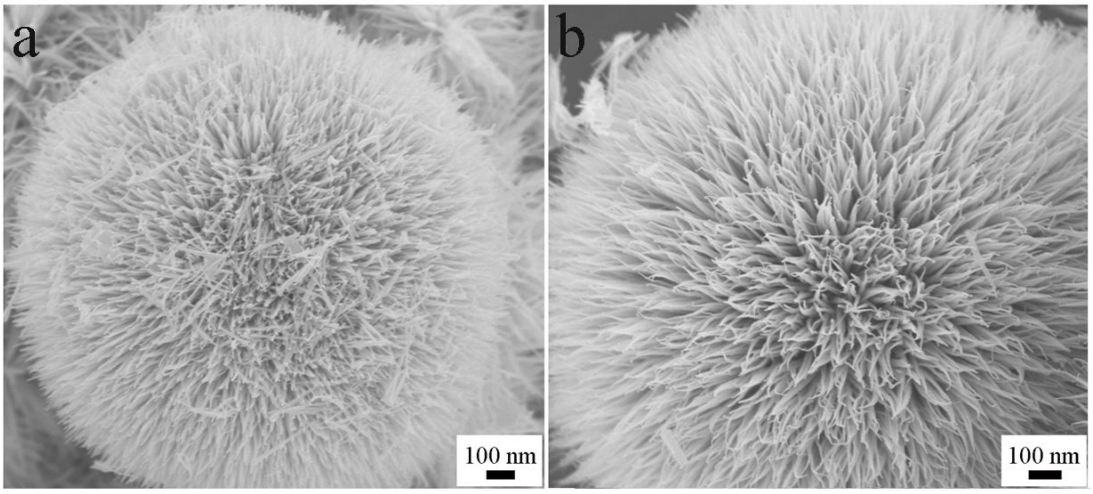

Figure S1. (a) SEM image of $NiCo_2O_4$; (b) SEM image of N-doped $NiCo_2O_4$.

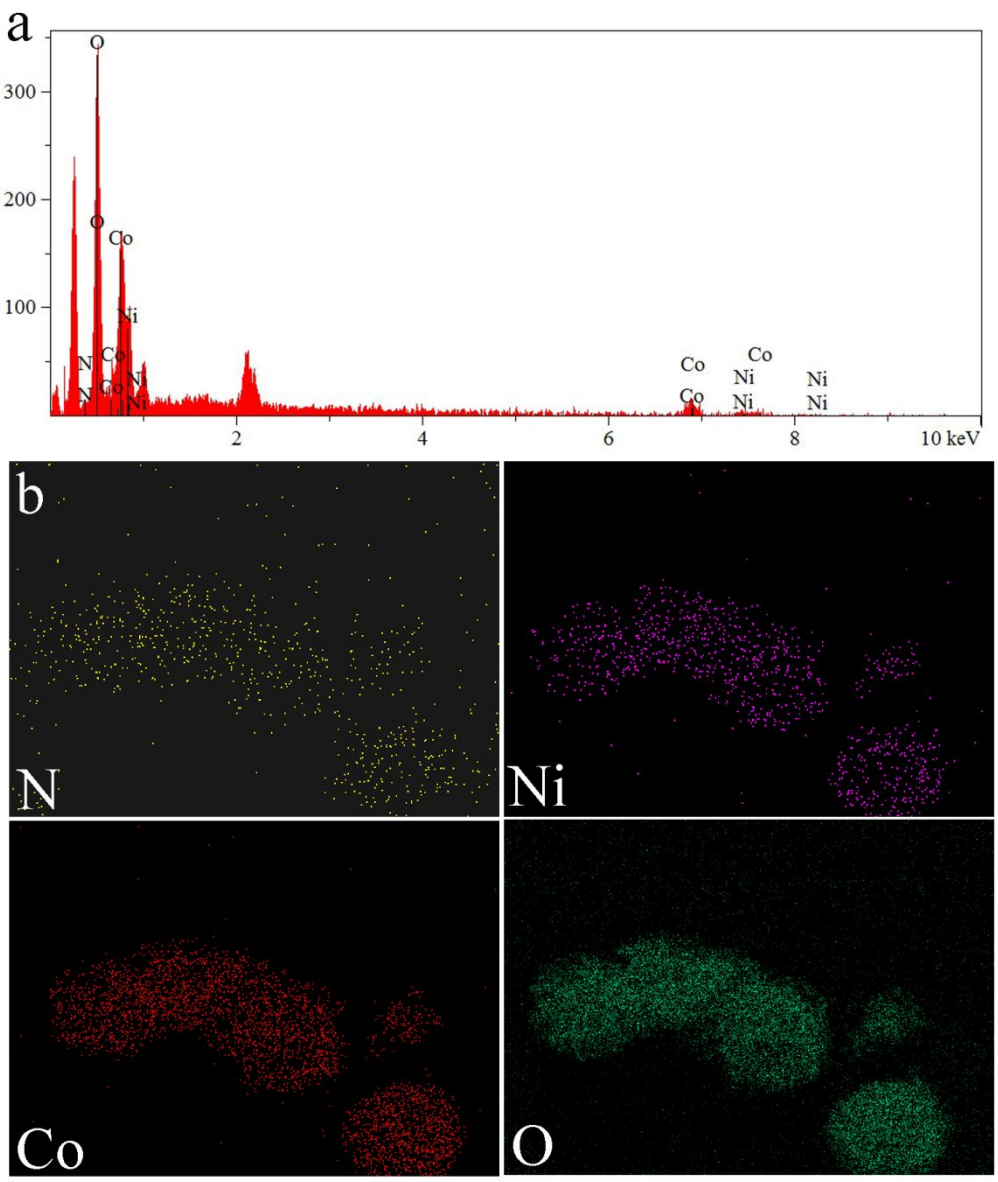

Figure S2. (a) EDS spectrum of N-doped $NiCo_2O_4$; (b) The corresponding elemental mappings of N, Ni, Co and O of the N-doped $NiCo_2O_4$.

Table S1 The contents of N, Ni, Co and O of the N-doped $NiCo_2O_4$.

Component	Contents (wt.%)
N	0.60
O	25.18
Co	46.95
Ni	27.27
Total	100

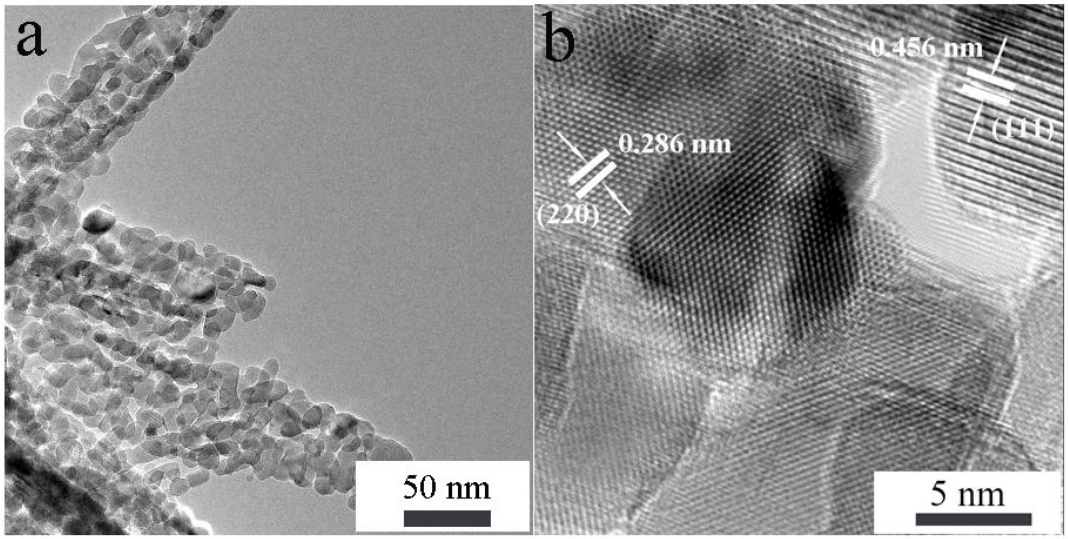

Figure S3. (a) TEM image and (b) HRTEM image of $NiCo_2O_4$.

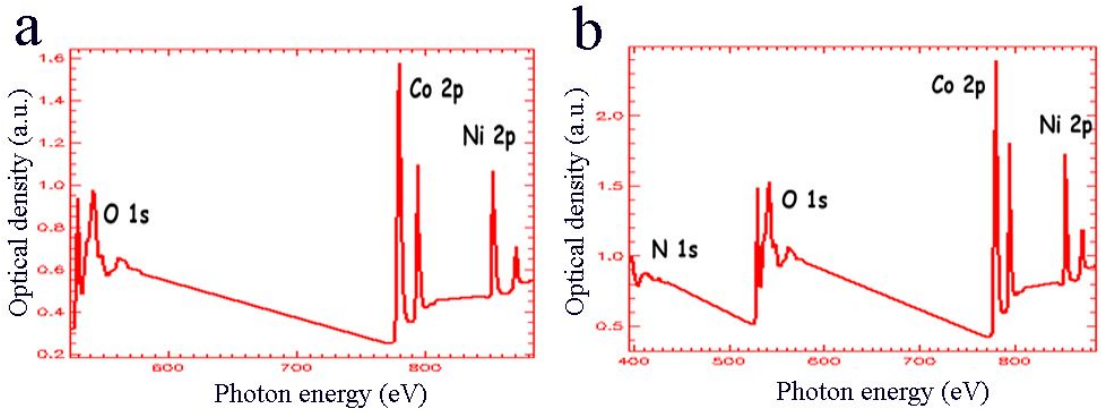

Figure S4. The whole XANES spectra of (a)$NiCo_2O_4$ and (b) N-doped $NiCo_2O_4$.

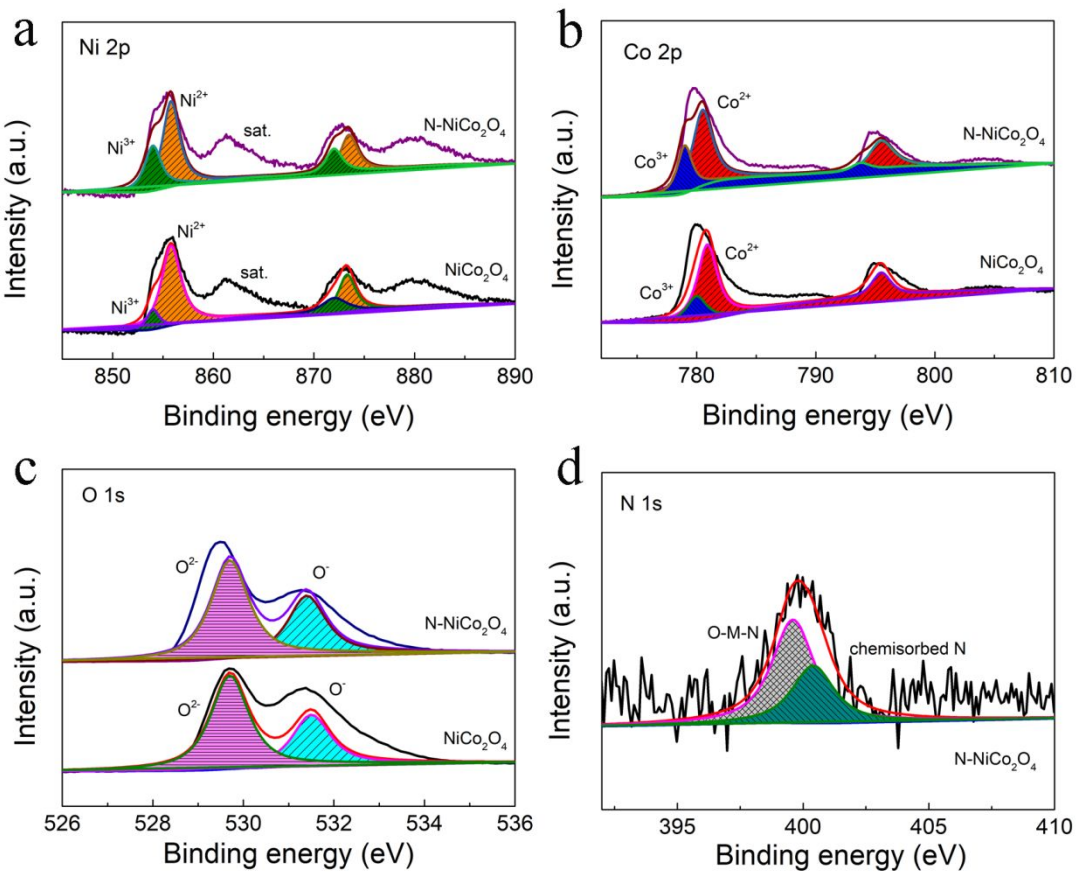

Figure S5. XPS spectra of $NiCo_2O_4$ and N-$NiCo_2O_4$: (a) Ni 2p spectra, (b) Co 2p spectra, (c) O 1s spectra, (d) N 1s spectrum.

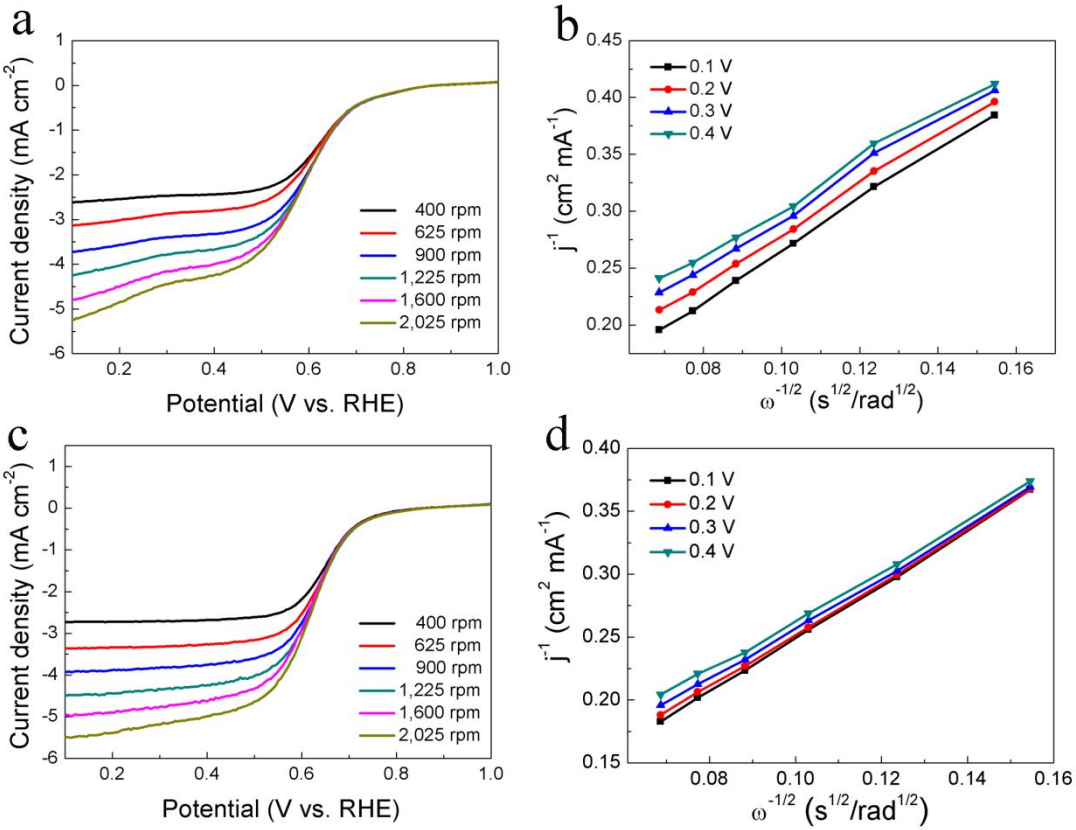

Figure S6. (a) LSV curves of $NiCo_2O_4$ at different rotating speeds; (b) the corresponding K-L plots at different potentials; (c) LSV curves of N-$NiCo_2O_4$ at different rotating speeds; (d) the corresponding K-L plots at different potentials.

Double layer capacitance (C_{dl}) of different electrodes was measured to estimate the effective electrochemical active surface area (ECSA) of the catalysts. CVs have been operated from 0.92 to 1.02 V (*vs.* RHE) in 0.1M KOH at different scan rates. The ECSA of the catalysts can be calculated according to the equal: ECSA $=C_{dl}/C_s$ where C_s is the specific capacitance of the sample. We use general C_s = 0.05 mF cm^{-2} in 0.1M KOH.[S1] From Figure S7, it can be calculated that N-doped $NiCo_2O_4$ has a bigger electrochemically active surface area of 26.1 cm^2 than that of $NiCo_2O_4$ (22 cm^2).

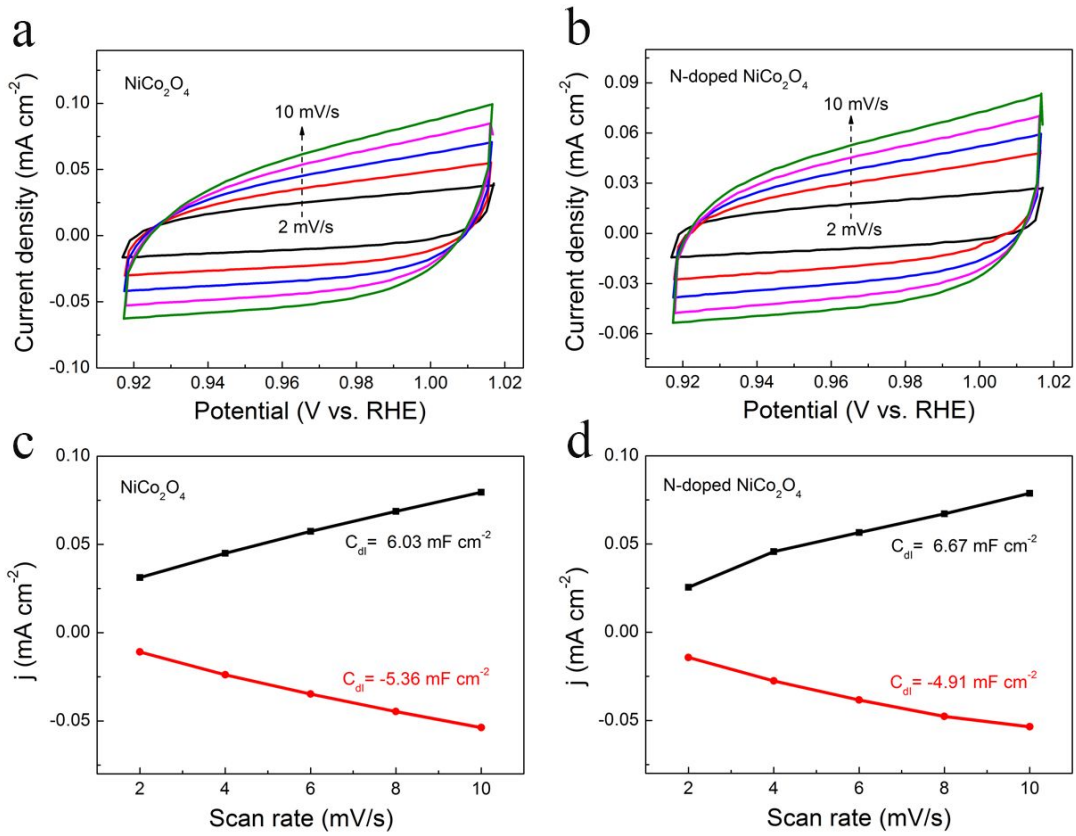

Figure S7. The cyclic voltammetry curves in the non-faradaic region at various scan rates for (a) $NiCo_2O_4$ and (b) N-doped $NiCo_2O_4$; Current-scan rates of the samples: (c) $NiCo_2O_4$ and (d) N-doped $NiCo_2O_4$.

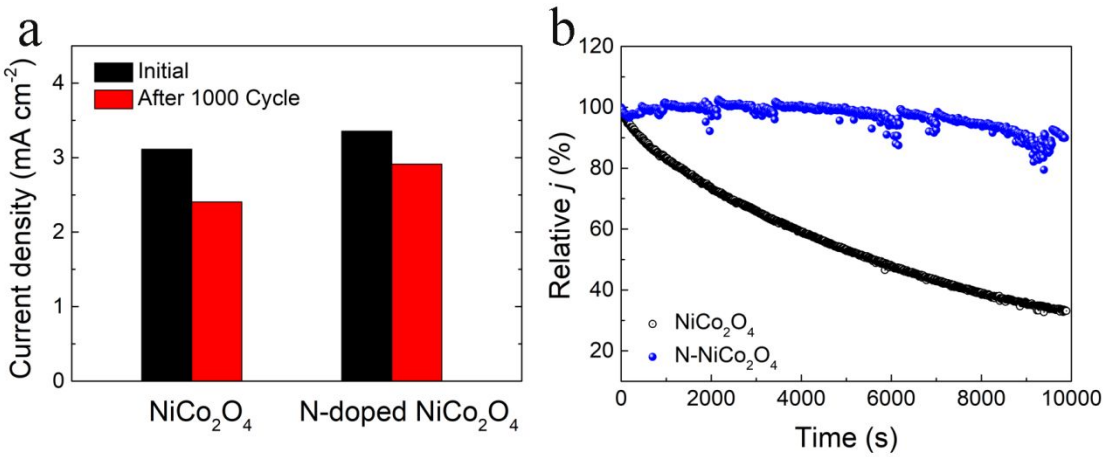

Figure S8. (a) Current densities at 0.5 V (*vs.* RHE) before and after 1000 cycles for $NiCo_2O_4$ and N-doped $NiCo_2O_4$; (b) Chronoamperometric response at 1.65V (*vs.* RHE) for $NiCo_2O_4$ and N-doped $NiCo_2O_4$.

Table S2 Comparison of the electrochemical performance of flexible zinc-air batteries with different catalysts

Catalyst	Current density	Battery performance	Potential gap (V)	Refs.
N-doped $NiCo_2O_4$	5 mA cm^{-2}	Galvanostatic test for 53 h	0.75	This work
Co_3O_4/CC	2 mA cm^{-2}	Galvanostatic test for 10 h	0.92	S2
Co_3O_4	no mention	Galvanostatic test for 35 h	0.85	S3
NCNF	2 mA cm^{-2}	Galvanostatic test for 6 h	0.78	S4
o-CC-H_2	1 mA cm^{-2}	Galvanostatic test for 30 min	0.97	S5
Co_3O_4/$LaNiO_3$/CNTs	5 mA g^{-1}	Galvanostatic test for 10 h	0.69	S6
CNT sheets	1 A g^{-1}	Galvanostatic test for 30 h	0.85	S7
Co_3O_4/N-rGO	3 mA cm^{-2}	Galvanostatic test for 25 h	0.80	S8

References

(S1) Fu, Y.; Yu, H.; Jiang, C.; Zhang, T.; Zhan, R.; Li, X,W.; Li, J,F.; Tian, J,H.; Yang, R,Z. NiCo Alloy Nanoparticles Decorated on N-Doped Carbon Nanofibers as Highly Active and Durable Oxygen Electrocatalyst. *Adv. Funct. Mater.* **2018**, 1705094.

(S2) Chen, X.; Liu, B.; Zhong, C.; Liu, Z.; Liu, J.; Ma, L.; Deng, Y.; Han, X.; Wu, T.; Hu, W.; Lu, J. Ultrathin Co_3O_4 Layers with Large Contact Area on Carbon Fibers as High-Performance Electrode for Flexible Zinc-Air Battery Integrated with Flexible Display. *Adv. Energy Mater.* **2017**, *7*, 1700779.

(S3) Fu, J.; Zhang, J.; Song, X.; Zarrin, H.; Tian, X.; Qiao, J.; Rasen, L.; Lib, K.; Chen, Z. A Flexible Solid-State Electrolyte for Wide-Scale Integration of Rechargeable Zinc-Air Batteries. *Energy Environ. Sci.* **2016**, *9*, 663-670.

(S4) Liu, Q.; Wang, Y.; Dai, L.; Yao, J. Scalable Fabrication of Nanoporous Carbon Fiber Films as Bifunctional Catalytic Electrodes for Flexible Zn-Air Batteries. *Adv. Mater.* **2016**, *28*, 3000-3006.

(S5) Wang, H.; Tang, C.; Wang, B.; Li, B.; Cui, X.; Zhang, Q. Defect-Rich Carbon Fiber Electrocatalysts with Porous Graphene Skin for Flexible Solid-State Zinc-Air Batteries. *Energy Storage Mater.* **2018**, *15*, 124-130.

(S6) Fu, J.; Lee, D.; Hassan, F.; Yang, L.; Bai, Z.; Park, M.; Chen, Z. Flexible High-Energy Polymer-Electrolyte-Based Rechargeable Zinc-Air Batteries. *Adv. Mater.* **2015**, *27*, 5617-5622.

(S7) Xu, Y.; Zhang, Y.; Guo, Z.; Ren, J.; Wang, Y.; Peng, H. Flexible, Stretchable, and Rechargeable Fiber-Shaped Zinc-Air Battery Based on Cross-Stacked Carbon Nanotube Sheets. *Angew. Chem. Int. Ed.* **2015**, *54*, 15390-15394.

(S8) Li, Y.; Zhong, C.; Liu, J.; Zeng, X.; Qu, S.; Han, X.; Deng, Y.; Hu, W.; Lu, J. Atomically Thin Mesoporous Co_3O_4 Layers Strongly Coupled with N-rGO Nanosheets as High-Performance Bifunctional Catalysts for 1D Knittable Zinc-Air Batteries. *Adv. Mater.* **2018**, *30*, 1703657.